

16 Abstract

17 A number of devastating wildfires occurred in southeast Australia on 7 February 2009,
18 colloquially known as Black Saturday. Atmospheric responses to this extreme fire event are
19 investigated here with a focus on convective processes associated with fire activity (i.e.,
20 pyroconvection). We examine six different fire complexes on Black Saturday, finding three
21 clearly distinct pyrocumulonimbus storms, the largest of which reached heights of 15 km on that
22 day and generated hundreds of lightning strokes. The first lightning stroke was recorded near the
23 largest fire complex five hours after fire ignition. One of the pyrocumulonimbus storms was
24 initiated close to midnight due to mesoscale influences, consistent with extreme fire behavior
25 observed at that time for that particular fire. As another example of fire-atmosphere interactions,
26 a fire that started late on Black Saturday is examined in relation to ignition caused by pyrogenic
27 lightning, with implications for understanding the maximum rate of spread of a wildfire. Results
28 are discussed in relation to another pyrocumulonimbus event associated with the 2003 Canberra
29 fires. Our findings are intended to provide a greater understanding of pyroconvection and fire-
30 atmosphere feedback processes, as well as help enhance wildfire response capabilities. We also
31 demonstrate the potential for using lightning, radar and satellite remote-sensing in combination
32 with thermodynamic analyses as well as synoptic and mesoscale dynamics to provide enhanced
33 real-time guidance for dangerous fire conditions associated with pyroconvection, as well as for
34 the risk of new fire ignitions from pyrogenic lightning.

35 1. Introduction

36 The fire regime of southern Australia is notable for the extremely dangerous conditions
37 that can sometimes occur during the austral summer [Luke and McArthur, 1978; Russell-Smith *et*
38 *al.*, 2007; Bradstock, 2010; Sullivan *et al.*, 2012; Murphy *et al.*, 2013]. Extreme fire-weather
39 conditions on Black Saturday (7 February 2009) near Melbourne in southeast Australia led to the
40 occurrence of wildfires that killed 173 persons, destroyed over 2,000 homes, burnt more than
41 450,000 ha and resulted in losses of over four billion Australian dollars [VBRC, 2010].

42 This event involved the combined influence of a number of extreme weather features. No
43 precipitation was recorded in the four weeks leading up to Black Saturday at the Melbourne
44 Airport observing station, with a strong anticyclone dominating southeastern Australia's weather
45 in the week prior to Black Saturday leading to a deep airmass of very hot air over this region
46 [BoM, 2009]. On Black Saturday, there was an approaching cold front southwest of this region
47 associated with a low pressure system further to the south as well as a high pressure system to
48 the east (Fig. 1). This set of synoptic features typifies many of the historical extreme fire events
49 in this region [Reeder and Smith, 1987; Mills, 2005a; Fiddes *et al.*, 2015; Reeder *et al.*, 2015].
50 The approaching cold front resulted in strong northwesterly winds that transported extremely hot
51 and dry air to the region near Melbourne from further inland, with the maximum temperature in
52 Melbourne reaching 46.4°C – the highest recorded from 154 years of record [BoM, 2009]. The
53 resultant extreme wind, heat, low humidity and fuel moisture [Sullivan and Matthews, 2013] on
54 Black Saturday combined to produce fire danger ratings reported to be as extreme as any in the
55 historical record for southeast Australia [BoM, 2009]. Furthermore, a wind change associated
56 with a surface trough ahead of the cold front (Fig. 1) passed over the fire region during the late
57 afternoon [BoM, 2009], leading to extremely dangerous fire behavior in terms of observed
58 intensity, rate of spread and spotting (i.e., the development of new fires, known as spot-fires,
59 ignited by burning debris transported by the fire plume) [Cruz *et al.*, 2012].

60 In addition to synoptic-scale conditions such as pre-frontal troughs and blocking highs
61 (e.g., Fig. 1, as well as discussed in various previous studies [Mills, 2005a; Mills, 2008; Potter,
62 2012a; Engel *et al.*, 2013; Reeder *et al.*, 2015]), dangerous fire behavior can also be associated
63 with localized convective processes that can increase near-surface wind speed and directional
64 variability thereby influencing fire rate of spread and intensity [Haines, 1988; Rothermel, 1991;
65 Banta *et al.*, 1992; Goens and Andrews, 1998; Potter, 2012a,b; Peterson *et al.*, 2015].
66 Convective processes can also lead to strong updrafts that increase the risk of spot-fire
67 occurrences [Cheney and Bary, 1969; Ellis, 2010; Koo *et al.*, 2010; Potter *et al.*, 2012b].
68 Furthermore, the heat, moisture and aerosol release from a fire can influence the fire plume
69 [Cunningham and Reeder, 2009; Luderer *et al.*, 2009; Clements *et al.*, 2010, Potter, 2012a,b;
70 Tosca *et al.*, 2015] and lead to the formation of convective clouds known as pyrocumulus
71 (pyroCu), or pyrocumulonimbus (pyroCb) in the case of the more intense systems such as those
72 observed on Black Saturday [BoM, 2009; VBRC, 2010; Field *et al.*, 2016]. A conceptual model,
73 based on observations in Western North America, also highlights the importance of atmospheric
74 conditions throughout the troposphere for pyroCb development [Peterson *et al.*, 2016]. PyroCbs
75 can sometimes produce lightning, referred to as pyrocumulus electrification or pyrogenic
76 lightning [Fernandez *et al.*, 2006; Lang and Rutledge, 2006; Rosenfeld *et al.*, 2007; Johnson *et*
77 *al.*, 2014; Lang *et al.*, 2014], and other potentially dangerous phenomena such as hail and
78 tornados [Fromm *et al.*, 2006; Cunningham and Reeder, 2009; McRae *et al.*, 2013].

79 The analysis presented here uses observations from a range of sources, including a
80 network of lightning detectors, ground-based radars, satellite imagery and station observations.
81 Fire-atmosphere interactions are examined, focusing on pyroCb behavior and associated
82 lightning activity. A new fire caused by pyrogenic lightning ignition, and the determinate factors
83 associated with this occurrence, are examined here for the first time in the literature. A second
84 southeast Australian pyroCb event, associated with the Canberra fires during January 2003, is
85 examined with respect to electrification and contrasted with Black Saturday. Results are
86 discussed in relation to improved model guidance and real-time intelligence for dangerous fire
87 conditions associated with pyroCbs.

88 2. Data and Methods

89 Figure 2 presents a map of southeast Australia showing features of relevance to this
90 study. This includes highlighting the regions of focus for the Black Saturday and Canberra fire
91 events, respectively, as well as the cities of Melbourne and Canberra and the locations of radars
92 from which data were obtained for use in this study.

93 Lightning observations were obtained from the commercial provider Global Position and
94 Tracking System Pty. Ltd. Australia (GPATS). The observations are based on the time of arrival
95 of the electromagnetic disturbance propagating away from the lightning discharge as recorded at
96 a network of ground-based radio receivers [Cummins and Murphy, 2009] and contain
97 information about the current magnitude and polarity, as well as the time and location of
98 individual lightning strokes, noting that a single lightning flash as seen by a human eye can
99 sometimes contain multiple lightning strokes (i.e., flash multiplicity). The detection efficiency of
100 the GPATS system varies temporally (e.g., due to ongoing changes in the hardware and software
101 used by the commercial provider of these data), spatially (e.g., due to proximity to receivers) and
102 between different types of lightning (e.g., for cloud-to-ground strokes or cloud-to-cloud strokes)
103 [Kuleshov *et al.*, 2006]. Consequently, the number of lightning strokes recorded by the GPATS

104 system is used throughout this study as a lower bound measure of the total lightning strokes that
105 occurred (i.e., the sum of the number of cloud-to-ground and cloud-to-cloud lightning strokes).

106 Data from three weather radars are used here to examine the Black Saturday fire event,
107 located at Laverton (37.9°S, 144.8°E) in the city of Melbourne, Yarrowonga (36.0°S, 146.0°E)
108 about 250 km northeast of Melbourne and Bairnsdale (37.8°S, 147.6°E) about 250 km east of
109 Melbourne. These data are examined here for times starting from 1800 LT, noting that the
110 Laverton radar was inoperable prior to 1806 LT due to the extreme heat. A fourth weather radar
111 is used to examine the Canberra fires, located at Captains Flat (35.6° S, 149.5° E) about 50 km
112 southeast of Canberra in southeast Australia, with the Canberra pyrocumulonimbus event on 18
113 January 2003 selected here for comparison with Black Saturday due to the severe thunderstorm
114 characteristics that were observed in association with that event [Fromm *et al.*, 2006, 2012; Mills
115 and McCaw, 2010; McRae *et al.*, 2013, 2015]. Reflectivity data are used to derive echo-top
116 altitudes, based on a 5 dBZ threshold, with prior radar analyses of pyroCbs [Fromm *et al.*, 2006,
117 2012; Rosenfeld *et al.*, 2007] showing how echo-top data are informative for examining both the
118 internal structure and the convective injection height of pyroCb events. The radar echoes come
119 not only from cloud hydrometeors, but also from debris lofted by the fires [Jones, 1950; Lindley
120 *et al.*, 2010; Baum *et al.*, 2015].

121 Active fire observations are obtained from the Moderate Resolution Imaging
122 Spectroradiometer (MODIS) on the Terra and Aqua satellites [Giglio *et al.*, 2009]. There were
123 three satellite overpasses for the fire region on the afternoon and evening of Black Saturday,
124 occurring for Aqua during the hour of 1500 Local Time (LT: 11 hours ahead of UTC, including
125 1 hour daylight saving) and for Terra during the hour of 2300 LT on 7 February 2009, as well as
126 for Aqua during the hour of 0200 LT on 8 February 2009.

127 A gridded analysis of precipitation observations is used from the Australian Water
128 Availability Project (AWAP) [Jones *et al.*, 2009], available on a 0.05° grid in both latitude and
129 longitude, based on daily accumulated precipitation totals for the 24-hour period to 0900 LT
130 each day. This grid is also used for the aggregation and analysis of the other datasets considered
131 throughout this study (i.e., the lightning, radar and active fire observations), as these other
132 datasets are available at finer spatial and temporal resolutions than the AWAP data.

133 3. Results

134 3.1. Black Saturday observations

135 Figure 3 shows maps of fire, lightning and precipitation observations on Black Saturday,
136 with the domain of these maps as highlighted in Fig. 2. Six notable fire events on that day are
137 listed, with the largest being the Kinglake complex. These fire events were all ignited on Black
138 Saturday, with the exception of the Bunyip fire which had been ignited a few days previously but
139 grew rapidly on Black Saturday due to the extreme fire weather conditions on that day (for
140 details, see [VBRC, 2010]). The Kinglake complex comprises a merging of the Kilmore East fire
141 and the Murrindindi fire which started on Black Saturday at around 1146 LT and 1445 LT,
142 respectively, with the Kilmore East fire being the most significant of the fires on Black Saturday
143 (resulting in 70% of the fatalities on that day and burning about 100,000 ha during the first 12
144 hours after ignition) [VBRC, 2010; Cruz *et al.*, 2012]. The strongest lightning activity occurred
145 southeast (i.e., downwind) of the Kinglake fire complex, with some other lightning activity in the
146 broader region away from the fire events. Relatively little precipitation occurred in this region on

147 Black Saturday, with only a small region of up to 4 mm precipitation occurring southeast of the
148 Kinglake complex.

149 Figure 4 shows radar echo-top heights at hourly intervals, for heights above 5 km, with
150 the values representing the highest value recorded during that hour. The echo-tops have
151 maximum heights of 15 km during the hour of 1900 LT over the Kinglake fire complex and
152 extending towards the southeast. This was during the period of most extreme fire behavior, with
153 *Cruz et al.* [2012] reporting that the area affected by fire during the hour of 1800 LT
154 (approximately 63,000 ha) was more than double the entire area burned by the fires prior to this
155 time. *Cruz et al.* [2012] also report that the burn dynamics during the hour of 1900 LT were
156 similar to those during the hour of 1800 LT, with somewhat weaker fire propagation from 2000
157 LT onwards. In addition to the Kinglake fire plume, a number of other plumes are evident from
158 the radar observations. For example, the Dargo fire plume has echo-top heights of about 12 km
159 during the hour of 1800 LT (Fig. 4a, around 37.0°S and 147.5°E) and somewhat lower values in
160 subsequent hours. The Beechworth fire plume is also clearly apparent, reaching heights of 10 km
161 during the hours near midnight LT (Fig. 4e,f,g, around 36.5°S and 147.0°E).

162 3.2. Temporal evolution of the lightning activity

163 Figure 5 shows the temporal evolution of the observed lightning activity as well as active
164 fire observations. The first lightning stroke was recorded at 1650 LT in the region where the
165 pyroCb occurred for the Kinglake fire complex, with lightning activity during the hour of 1700
166 LT also occurring only in that region, indicating the influence of the fire activity on initiating the
167 lightning activity.

168 The majority of lightning activity during the hour of 1800 LT (Fig. 45d) is clustered
169 around the Kinglake fire complex, as well as some lightning strokes to the northwest mapping
170 out a line similar to the location of the wind change at this time associated with the synoptic-
171 scale pre-frontal trough passing over the region at this time (see *Cruz et al.* [2012] and Fig. 1).
172 As the wind change progressed across this region it produced rising air masses above its leading
173 edge [*Engel et al.*, 2013], which plausibly provided the trigger for initiating deep convection (as
174 indicated by the lightning activity) in locations away from the fire activity. During the following
175 two hours (1900 LT and 2000 LT), lightning activity is only sustained in the region around the
176 Kinglake pyroCb (a roughly elliptical region with a major axis of about 100 km in length), with
177 no lightning observed in surrounding regions, indicating the ongoing interaction between the
178 Kinglake fire complex and the atmospheric processes throughout this time period.

179 The first fire ignition of the Kinglake complex occurred shortly before 1200 LT [*Cruz et*
180 *al.*, 2012], five hours prior to the first lightning observed in this region on Black Saturday. Such
181 a short time interval from fire ignition to lightning generation offers broad implications for
182 understanding fire behavior exacerbation rates, given that previous studies have shown that rapid
183 and deep convection may be associated with dangerous variations in fire behavior (e.g., *Potter et*
184 *al.* [2012b]). To put this time interval for Black Saturday into a more general context, a study of
185 multiple pyroCb events in North America [*Peterson et al.*, 2016] reported that "generally
186 speaking, pyroCb can occur at any point in a fire's lifetime, occasionally as early as the first 48
187 hours."

188 In addition to the Kinglake complex, the other fire event with lightning activity strongly
189 clustered around it is the Beechworth fire. This fire was ignited at about 1800 LT on Black

190 Saturday, with lightning activity in this region first observed at about midnight LT (six hours
191 after ignition) and persisting until about 0200 LT the following morning (Fig. 5j,k, around
192 36.5°S and 147.5°E). The Incident Controller for managing the Beechworth fire observed
193 extreme fire behavior close to midnight, including reporting a “firestorm” approaching the town
194 of Mudgegonga (around 36.5°S, 146.9°E) [VBRC, 2010]. These lightning data (Fig. 5) indicate a
195 significant change in convective processes within the Beechworth pyroCbs around midnight LT,
196 consistent with the timing of the extreme fire behavior observed by the response personnel.

197 *Engel et al.* [2013] showed that shortly after 2300 LT a mesoscale bore passed over the
198 Beechworth fire region introducing variability in atmospheric conditions at short spatial and
199 temporal scales which can have large influences on fire danger. Rising air masses above the
200 leading edge of the bore (as shown by *Engel et al.* [2013]) is suggested here to have likely helped
201 initiate the deep pyroconvective processes required to electrify the Beechworth pyroCb,
202 consistent with the initiation of the lightning activity around midnight LT. However, the bore is
203 only one factor that helped initiate this lightning, given that lightning is not observed in the
204 region away from the Beechworth fire plume, thereby indicating strong fire-atmosphere
205 interactions in this case.

206 3.3. Fire ignition from pyrogenic lightning

207 A new fire can be seen during the hour of 0200 LT on 8 February 2009 (Fig. 5l, around
208 146.5°E and 38.0°S) that was not observed in previous satellite overpasses. This fire is listed as
209 caused by lightning on Black Saturday in the Victorian State Government records of fire events
210 based on post-fire investigations by response personnel. These records refer to this fire event as
211 the 'East Tyers - Thompson' fire and state that it started at 1800 LT on Black Saturday due to
212 lightning ignition. Complementary to the post-fire investigations, the analysis of remotely-sensed
213 data presented here demonstrates a high risk of fire ignition from lightning in that region,
214 including due to the high concentration of lightning activity produced by the Kinglake pyroCb in
215 the region where this new fire occurred (Fig. 5). Another important factor in determining
216 whether or not a sustained fire will develop following a lightning ignition is the amount of
217 precipitation that accompanies the lightning activity, with lightning accompanied by relatively
218 little precipitation known as dry-lightning [*Fuquay et al.*, 1972; *Latham*, 1991; *Rorig and*
219 *Ferguson*, 1999]. The risk of fire occurrence from a lightning ignition in this region of southeast
220 Australia is higher than average if less than about 3 mm of precipitation occurs and lower than
221 average if more than about 5 mm of precipitation occurs [*Dowdy and Mills*, 2012a,b].
222 Consequently, the relatively low amount of precipitation (Fig. 3), coupled with the pre-existing
223 dryness of the fuels on Black Saturday [*Sullivan and Matthews*, 2013], indicate a substantial risk
224 of sustained fire ignition from the observed lightning activity in this region (Fig. 5).

225 An additional consideration in relation to the cause of this new fire is that it occurred
226 about 100 km downwind of the Kinglake fire complex. This is too far for ember transport by the
227 fire plume to be the cause of ignition, even considering the extreme ember transport distances
228 observed on Black Saturday which resulted in spot-fires occurring up to about 33 km ahead of
229 the main fire front [*Cruz et al.*, 2012].

230 3.4. Comparison with Canberra fire event

231 A number of Australian pyroCb events have been documented in recent years [*Fromm et*
232 *al.*, 2006, 2012; *Mills et al.*, 2010; *McRae et al.*, 2013, 2015]. The Canberra fire event on 18

233 January 2003 is particularly notable in that it resulted in pyroCb that injected smoke into the
234 stratosphere and perturbed stratospheric aerosol loading for at least two months [Fromm *et al.*,
235 2006]. Figure 6 shows the broad-scale meteorology on that day, including a large high in the
236 Tasman Sea to the east of the continent as well as a mid-latitude trough over southeast Australia
237 with a cold front further to the south of that region. Lightning activity associated with this event
238 has not previously been examined in the literature. However, hail activity and a tornado (a non-
239 super-cell type of tornado) associated with this pyroCb have been documented [Fromm *et al.*,
240 2006; Cunningham and Reeder, 2009; McRae *et al.*, 2013], noting that tornado or hail
241 observations provide a means of defining severe thunderstorm occurrence (e.g., based on
242 Australian Bureau of Meteorology operational practices). Given these severe thunderstorm
243 characteristics of the Canberra event, it is selected here for examination in comparison with
244 Black Saturday.

245 Figure 7 presents observations similar to those shown in Figures 3 and 4, but for the
246 region around Canberra on 18 January 2003. These include satellite observations of active fires,
247 precipitation data and lightning observations, as well as echo-top heights (from the Captains Flat
248 radar about 50 km southeast of Canberra).

249 Lightning activity was not observed in the region near the fire activity, with only four
250 lightning strokes recorded over 100 km northeast of Canberra (Fig. 7b), noting that this lightning
251 activity was not downwind of the fires and occurred too far away to be associated with the fire
252 activity. Additionally, no thunder was recorded as being heard on this day by the Canberra office
253 of the Bureau of Meteorology in their thunderstorm observation records.

254 Although no lightning was observed in association with the Canberra pyroCb event, it
255 could be possible that lightning activity occurred but was not detected. For example, a case
256 occurred in the USA where the National Lightning Detection Network (NLDN) observed no
257 lightning activity associated with a pyroCb, even though cloud-to-cloud (intra-cloud) lightning
258 was observed by locally deployed lightning sensors [Lang *et al.*, 2014]. However, even
259 considering the possibility that lightning did occur for the Canberra event but was not detected
260 by the GPATS network (e.g., relatively weak intra-cloud lightning), there is a clear difference
261 between Black Saturday and the Canberra event in terms of the characteristics of the lightning
262 activity. This is potentially associated with the Canberra event having extremely dry conditions
263 in some parts of the troposphere as compared to Black Saturday [Cunningham and Reeder, 2009;
264 McCaw *et al.*, 2009] including the occurrence of a mid-tropospheric dry band for the Canberra
265 event that led to abrupt surface drying resulting from vertical mixing [Mills 2005b, 2008].

266 The relative dryness of the mid-troposphere for the Canberra event as compared to Black
267 Saturday is indicated by radiosonde observations during the middle of the day from Wagga
268 Wagga (35.11° S, 147.36° E: about 180 km west of Canberra) for the Canberra fire event and
269 from Melbourne Airport for Black Saturday (Fig. 8). For example, the dewpoint temperature
270 from 800 hPa to 700 hPa ranges from about -2°C to -7°C at Wagga Wagga as compared to
271 values from about 0°C to 3°C at Melbourne Airport. The thermodynamic environmental
272 conditions for the two cases show some broad similarities to each other, including an 'inverted v'
273 profile characterized by decreasing dewpoint depression with increasing height above the
274 surface, consistent with the conceptual model of Peterson *et al.* [2016] of a dry and deep mixed
275 layer with ambient mid-level moisture as typical factors associated with intense pyroCb
276 development. The lifted condensation level (LCL) is 640 hPa for Wagga Wagga and 620 hPa for
277 Melbourne Airport. Above the LCL at around 500-600 hPa, the dewpoint depression is larger for

278 Wagga Wagga (ranging from about 15°C to 25°C) than for Melbourne Airport (ranging from
279 about 5°C to 10°C), while noting that at around 400 hPa the dewpoint depression is higher for
280 Melbourne Airport than Wagga Wagga. Drier conditions for the Canberra event as compared to
281 Black Saturday are also indicated by the precipitation observations presented here, with no
282 precipitation recorded in the region near the Canberra fires (Fig. 7b), compared with 1-4 mm
283 precipitation in the region where the Kinglake pyroCb occurred (Fig. 3c).

284 Although both of these fire events had deep convection reaching the stratosphere, as well
285 as the ‘inverted v’ type of atmospheric profile (Fig. 8), the lightning data have illuminated a
286 dichotomy between these two extreme pyroconvection events. We have suggested here that drier
287 conditions in the lower and middle troposphere for the Canberra event as compared with Black
288 Saturday could have potentially been an unfavorable factor for the generation of lightning
289 activity, while acknowledging that there are a range of uncertainties associated with these
290 processes (e.g., associated with the relative amount of entrainment and detrainment at different
291 tropospheric levels that the surface parcel from the fire will experience as it is lifted). It is also
292 noted that the atmospheric profiles shown in Fig. 8 represent particular locations and times that
293 are not exactly coincident with the actual pyroCb development in each case. Consequently, care
294 is taken here to avoid making generalized conclusions based on these results from only two days
295 (i.e., for Black Saturday and the Canberra event). To further examine this apparent conundrum
296 that the lightning observations have highlighted, examinations of other similar cases throughout
297 the world are intended for greater understanding of the processes leading to electrified
298 pyroconvection.

299 **4. Discussion**

300 The analysis presented here provides evidence that extensive pyroCb activity occurred on
301 Black Saturday, including a number of distinct electrified pyroCb clusters, the largest of which
302 reached heights of around 15 km on that day. As noted by *Bannister* [2009, 2014], fire agencies
303 were very concerned about the potential for pyroCb formation on Black Saturday, even though
304 forecast models did not indicate a high risk of thunderstorm development, as normal model
305 thunderstorm guidance does not represent the heat and moisture release from the fire.
306 Consequently, pyroCb-specific model guidance (e.g., as could be developed based on coupled
307 fire-atmosphere modelling [*Clark et al.*, 1997; *Cunningham and Reeder*, 2009; *Potter* 2012b])
308 and real-time intelligence (e.g., based on improved remote sensing capabilities) would greatly
309 add to the forecaster service to fire agencies. The analysis presented here indicates considerable
310 potential to use a range of remotely-sensed data in fire management applications, including
311 combining lightning observations with ground-based radar and satellite observations for
312 improved pyroCb monitoring and modelling (e.g., nowcasting). Additionally, the Himawari-8
313 and Himawari-9 satellites recently launched by Japan provide imagery at 10-minute intervals
314 over a longitudinal region surrounding Japan that includes Australia [*Kurino*, 2012], representing
315 a considerable advance in remote sensing capabilities in this region.

316 Previous studies demonstrate significant changes in fire behavior in response to synoptic
317 conditions on Black Saturday including in response to the pre-frontal trough and associated
318 change in wind direction [BoM, 2009; VBRC, 2010; Cruz et al., 2012; Engel et al. 2013]. The
319 results presented here build on these findings in showing that there was a significant atmospheric
320 response to this change in fire behavior, including the occurrence of pyrogenic lightning activity
321 tightly clustered around the fire plume of the Kinglake complex. Additionally, the new fire

322 ignited by this pyrogenic lightning, examined in Section 3.3, further highlights the feedback
323 loops of influence between the atmosphere and fire behavior on Black Saturday associated with
324 these pyroconvective processes. In addition to indicating this strong coupling on Black Saturday
325 between the atmosphere and the fire activity, the lightning observations also suggest
326 considerable differences in pyroCb characteristics between Black Saturday and the Canberra fire
327 event. Differences between pyroCb events, such as for the Black Saturday and Canberra cases,
328 indicate considerable potential for improved understanding of pyroconvection based on
329 combining different data sets as presented here (including in relation to lightning, radar,
330 precipitation and satellite observations).

331 Complementary to previous studies focusing on the role of combustion-released moisture
332 and heat in driving pyroconvection [Cunningham and Reeder, 2009; Luderer *et al.*, 2009;
333 Clements *et al.*, 2010, Potter, 2012a,b; Tosca *et al.*, 2015], the results for Black Saturday
334 demonstrate that synoptic-scale dynamics are also important to consider, including in relation to
335 the initiation of deep pyroconvective processes: e.g., as occurred around the time of the pre-
336 frontal trough passing over the Kinglake fire region (examined in Section 3.2). In relation to
337 mesoscale dynamics, the initiation of deep convection around midnight LT for the Beechworth
338 pyroCb (as indicated by the lightning observations) does not match the mid-afternoon peak in the
339 severity of the near-surface fire weather conditions in this region [BoM, 2009; Cruz *et al.*, 2012],
340 whereas the occurrence of rising air masses above the leading edge of the bore that passed over
341 this region (as shown previously by Engel *et al.* [2015]) is consistent with the timing of the onset
342 of lightning activity close to midnight. In addition to mesoscale dynamics associated with this
343 bore, strong fire-atmosphere interactions likely also played a role in triggering this pyroCb, given
344 that lightning is not observed in the broader surrounding region away from the Beechworth fire
345 plume.

346 Fire ignition by pyrogenic lightning has been reported by fire management authorities for
347 a number of recent wildfires, including the Fort McMurray fire in Alberta, Canada, in May 2016
348 and the Waroona fire in January 2016 in Western Australia [Ferguson, 2016], however, this
349 phenomena has not previously been examined in the scientific literature. The examinations
350 presented here for Black Saturday demonstrate that fires ignited by lightning generated within
351 the fire plume can occur at much larger distances ahead of the main fire front—of the order of
352 about 100 km—than fires ignited by burning debris transported by the fire plume (up to about 33
353 km [Cruz *et al.*, 2012]), noting that this also has implications in relation to understanding the
354 maximum rate of spread of a wildfire.

355 The Black Saturday fire plumes were observed at stratospheric altitudes in the subsequent
356 days as detailed in a number of studies [Siddaway *et al.*, 2010; Pumphrey *et al.*, 2011; Glatthor
357 *et al.*, 2013] and although these studies did not examine the stratospheric injection event
358 specifically they all speculated that pyroCb activity was likely the cause. However, a remarkable
359 aspect of the pyroCb phenomenon is that it has often been overlooked and its effects
360 misattributed [Fromm *et al.*, 2010]. For example, de Laat *et al.* [2012] examined the Black
361 Saturday conditions and concluded that ‘extensive deep pyroconvection is not observed and
362 unlikely to have developed due to unfavorable meteorological conditions’ and proposed a
363 diabatic process for lofting between the middle troposphere and stratosphere. Hence it is
364 essential to fully explore events such as these to properly characterize the fire behavior, pyroCb
365 dynamics and resultant influence on conditions in the upper troposphere and lower stratosphere
366 (UTLS). It is also important to accurately characterize this transport process so that cloud,

367 chemistry and climate models have a firm basis on which to evaluate the pyrogenic source term,
 368 pathway from the boundary layer through cumulus cloud, and exhaust from the convective
 369 column.

370 A greater understanding of pyroCb activity is important, given that fire-atmosphere
 371 feedback processes can exacerbate the conditions associated with dangerous fire behavior. It is
 372 intended that our findings will have benefits for fire response capabilities, based on improved
 373 preparedness and real-time monitoring of the potential for dangerous fire conditions associated
 374 with pyroconvection. Additionally, understanding the combined effects of heat, moisture and
 375 aerosols on cloud microphysics is important for a range of weather and climate processes,
 376 including in relation to improved modelling and prediction capabilities.

377 **Acknowledgments**

378 This research was supported by the Australian Government's National Environmental Science
 379 Programme. Assistance provided by Michael Whimpey and Josh Soderholm with radar data is
 380 gratefully acknowledged. MODIS Active Fire Product data are available from the Land
 381 Processes Distributed Active Archive Center (LP-DAAC) using the EOS Data Gateway web
 382 interface (located at: <http://reverb.echo.nasa.gov>). Other data used here are available on request
 383 from the Australia Bureau of Meteorology. The authors would like to thank the anonymous
 384 reviewers for their insightful comments and suggestions that have contributed to improve this
 385 paper.

386 **References**

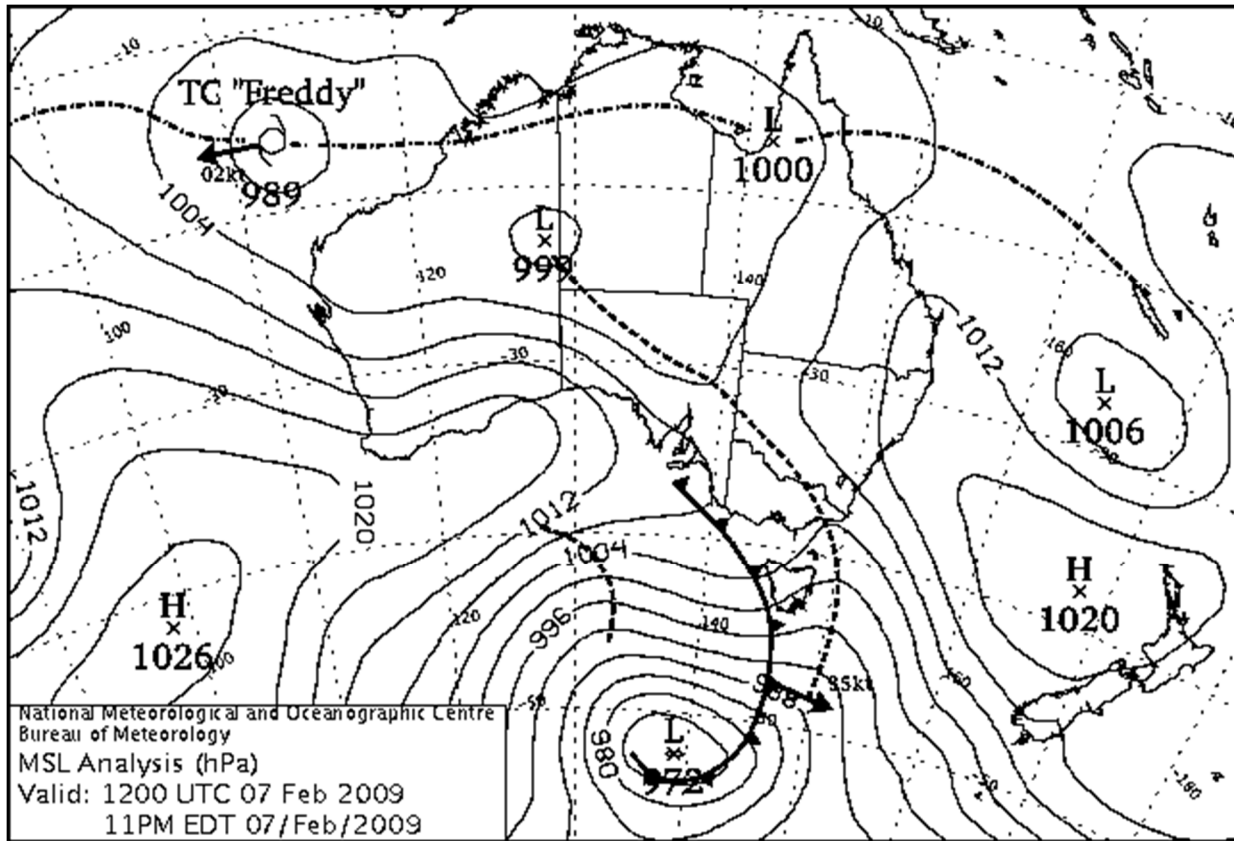
- 387 Bannister, T. (2009), Modelling challenges from the Black Saturday 2009 event, In 'Modelling
 388 and Understanding High Impact Weather': extended abstracts of the third CAWCR
 389 Modelling Workshop, pp 134. *Centre for Australian Weather and Climate Research*,
 390 Melbourne, Australia.
- 391 Bannister, T. (2014), Black Saturday 2009: A radar view of the Kilmore East fire, *CAWCR*
 392 *Research Letters*, Issue 11, 10-13pp, ISSN: 1836-5949.
- 393 Banta, R. M., L. D. Olivier, E. T., Holloway, R. A., Kropfli, B. W., Bartram, R. E., Cupp, and M.
 394 J. Post (1992), Smoke-column observations from two forest fires using Doppler lidar and
 395 Doppler radar, *J. Appl. Meteorol.*, 31(11), 1328-1349.
- 396 Baum, T. C., L. Thompson, and K. Ghorbani (2015), The Nature of Fire Ash Particles:
 397 Microwave Material Properties, Dynamic Behavior, and Temperature Correlation. *IEEE*
 398 *Journal of Selected Topics in Applied Earth Observations and Remote Sensing*, 8(2), 480-
 399 492.
- 400 Bradstock, R. A. (2010), A biogeographic model of fire regimes in Australia: current and future
 401 implications, *Global Ecology and Biogeography*, 19(2), 145-158.
- 402 Bureau of Meteorology (BoM) (2009), Meteorological aspects of the 7 February 2009 Victorian
 403 fires, an overview. Bureau of Meteorology report for the 2009 Victorian Bushfires Royal
 404 Commission, *Bureau of Meteorology*, Melbourne, Australia.
- 405 Cheney, N. P., and G. A. V. Bary (1969), The propagation of mass conflagrations in a standing
 406 eucalypt forest by the spotting process, In *Mass Fire Symposium* (pp. 10-12). Defense
 407 Standards Laboratory.

- 408 Clark, T. L., M. A. Jenkins, J. L. Coen, and D. R. Packham (1997), A coupled atmosphere-fire
409 model: Role of the convective Froude number and dynamic fingering at the fireline, *Int.*
410 *J. Wildland Fire*, 6(4), 177-190.
- 411 Clements, C. B. (2010), Thermodynamic structure of a grass fire plume, *Int. J. Wildland Fire*,
412 19(7), 895-902.
- 413 Cruz, M. G., A. L. Sullivan, J. S., Gould, N. C., Sims, A. J., Bannister, J. J., Hollis, R. J., and R.
414 J. Hurley (2012), Anatomy of a catastrophic wildfire: the Black Saturday Kilmore East
415 fire in Victoria, Australia, *Forest Ecology and Management*, 284, 269-285.
- 416 Cummins, K. L., and M. J. Murphy (2009), An overview of lightning locating systems: History,
417 techniques, and data uses, with an in-depth look at US NLDN, *IEEE Trans.*
418 *Electromagn. Compat.*, 51, 499-518.
- 419 Cunningham, P., and M. J. Reeder (2009), Severe convective storms initiated by intense wild
420 fires: Numerical simulations of pyrocumulonimbi and pyro-tornadogenesis, *Geophys.*
421 *Res. Lett.*, 36:L12812, DOI:10.1029/2009GL039262.
- 422 De Laat, A. T. J., D. C. Stein Zweers, and R. Boers (2012), A solar escalator: Observational
423 evidence of the self-lifting of smoke and aerosols by absorption of solar radiation in the
424 February 2009 Australian Black Saturday plume, *J. Geophys. Res. Atmos.*, 117(D4).
- 425 Dowdy, A. J., and G. A. Mills (2012a), Characteristics of lightning-attributed wildland fires in
426 south-east Australia, *Int. J. Wildland Fire*, 21(5), 521-524.
- 427 Dowdy, A. J., and Mills, G. A. (2012b), Atmospheric and fuel moisture characteristics associated
428 with lightning-attributed fires, *J. Appl. Meteorol. Climatol.*, 51, 2025-2037,
429 doi:10.1175/JAMC-D-11-0219.1.
- 430 Ellis, P. F. M. (2011), Fuelbed ignition potential and bark morphology explain the notoriety of
431 the eucalypt messmate 'stringybark' for intense spotting, *Int. J. Wildland Fire*, 20(7), 897-
432 907.
- 433 Engel, C. B., T. P. Lane, M. J. Reeder, and M. Rezny (2013), The meteorology of Black
434 Saturday, *Q. J. R. Meteorol. Soc.*, 139, 585-599.
- 435 Ferguson, E (2016), Reframing Rural Fire Management: Report of the Special Inquiry into the
436 January 2016 Waroona Fire. Public Service Commission, Government of Western
437 Australia (available from [https://publicsector.wa.gov.au/document/reframing-rural-fire-](https://publicsector.wa.gov.au/document/reframing-rural-fire-management-report-special-inquiry-january-2016-waroonafire)
438 [management-report-special-inquiry-january-2016-waroonafire](https://publicsector.wa.gov.au/document/reframing-rural-fire-management-report-special-inquiry-january-2016-waroonafire)).
- 439 Fernandes, W. A., I. R. Pinto, O. Pinto, K. M. Longo, and S. R. Freitas (2006), New findings
440 about the influence of smoke from fires on the cloud-to-ground lightning characteristics
441 in the Amazon region, *Geophys. Res. Lett.*, 33(20).
- 442 Fiddes, S. L., A. B. Pezza, and J. Renwick (2015), Significant extra-tropical anomalies in the
443 lead up to the Black Saturday fires, *Int. J. Climatol.*, 36(2), 1011-1018, DOI:
444 10.1002/joc.4387.
- 445 Field, R. D., M. Luo, M. Fromm, A. Voulgarakis, S. Mangeon, and J. Worden (2016),
446 Simulating the Black Saturday 2009 smoke plume with an interactive composition-
447 climate model: Sensitivity to emissions amount, timing, and injection height, *J. Geophys.*
448 *Res. Atmos.*, 121(8), 4296-4316.

- 449 Fromm, M., A. Tupper, D. Rosenfeld, R. Servranckx, and R. McRae (2006), Violent pyro-
450 convective storm devastates Australia's capital and pollutes the stratosphere, *Geophys.*
451 *Res. Lett.*, 33, L05815, doi:10.1029/2005GL025161.
- 452 Fromm, M., D. T. Lindsey, R. Servranckx, G. Yue, T. Trickl, R. Sica, P. Doucet, and S. Godin-
453 Beekmann, S. (2010), The untold story of pyrocumulonimbus, *Bull. Americ. Meteorol.*
454 *Soc.*, 91(9).
- 455 Fromm, M. D., R. H. D. McRae, J. J. Sharples, and G. P. Kablick III (2012), Pyrocumulonimbus
456 pair in Wollemi and Blue Mountains National Parks, 22 November 2006, *Australian*
457 *Meteorological and Oceanographic Journal*, 62(3), 117-126.
- 458 Fuquay, D. M., R. G. Baughman, A. R. Taylor, and R. G. Hawe (1967), Characteristics of seven
459 lightning discharges that caused forest fires, *J. Geophys. Res.*, 72(24), 6371-6373.
- 460 Giglio, L., T. Loboda, D. P. Roy, B. Quayle, and C. O. Justice (2009), An active-fire based
461 burned area mapping algorithm for the MODIS sensor, *Remote Sensing of Environment*,
462 113(2), 408-420.
- 463 Glatthor, N., M. Höpfner, K. Semeniuk, A. Lupu, P. I. Palmer, J. C. McConnell, J. W. Kaminski,
464 T. V. Clarmann, G. P. Stiller, B. Funke, and S. Kellmann (2013), The Australian
465 bushfires of February 2009: MIPAS observations and GEM-AQ model results, *Atmos.*
466 *Chem. Phys.*, 13(3), 1637-1658.
- 467 Goens, D. W., and O. L. Andrews (1998), Weather and fire behavior factors related to the 1990
468 Dude Fire near Payson, AZ, NWCG Wildland Fire Leadership Development Program.
- 469 Haines, D. (1988), A lower atmosphere severity index for wildland fire, *National Weather*
470 *Digest*, 13, 23-27.
- 471 Jones, R. F. (1950), Radar echoes from smoke, *Meteorological Magazine*, London, 79, p.89.
- 472 Jones, D., W. Wang, and R. Fawcett (2009), High-quality spatial climate datasets for Australia,
473 *Aust. Meteorol. Mag.*, 58, 233-248
- 474 Johnson, R. H., R. S. Schumacher, J. H. Ruppert Jr, D. T. Lindsey, J. E. Ruthford, & L.
475 Kriederman (2014), The Role of Convective Outflow in the Waldo Canyon Fire, *Mon.*
476 *Weath. Rev.*, 142(9), 3061-3080. Koo, E., P. J. Pagni, D. R. Weise, and J. P. Woycheese
477 (2010), Firebrands and spotting ignition in large-scale fires, *Int. J. Wildland Fire*, 19(7),
478 818-843.
- 479 Kuleshov, Y., D. Mackerras and M. Darveniza (2006), Spatial distribution and frequency of
480 lightning activity and lightning flash density maps for Australia, *J. Geophys. Res.*, 111,
481 D19105, doi:10.1029/2005JD006982.
- 482 Kurino, T. (2012), Future Plan and Recent Activities for the Japanese Follow-on Geostationary
483 Meteorological Satellite Himawari-8/9, AGU Fall Meeting Abstracts. Vol. 1.
- 484 Lang, T. J., and S. A. Rutledge (2006), Cloud-to-ground lightning downwind of the 2002
485 Hayman forest fire in Colorado, *Geophys. Res. Lett.*, 33(3).
- 486 Lang, T. J., S. A. Rutledge, B. Dolan, P. Krehbiel, W. Rison, and D. T. Lindsey (2014),
487 Lightning in wildfire smoke plumes observed in Colorado during summer 2012, *Mon.*
488 *Weath. Rev.*, 142(2), 489-507.

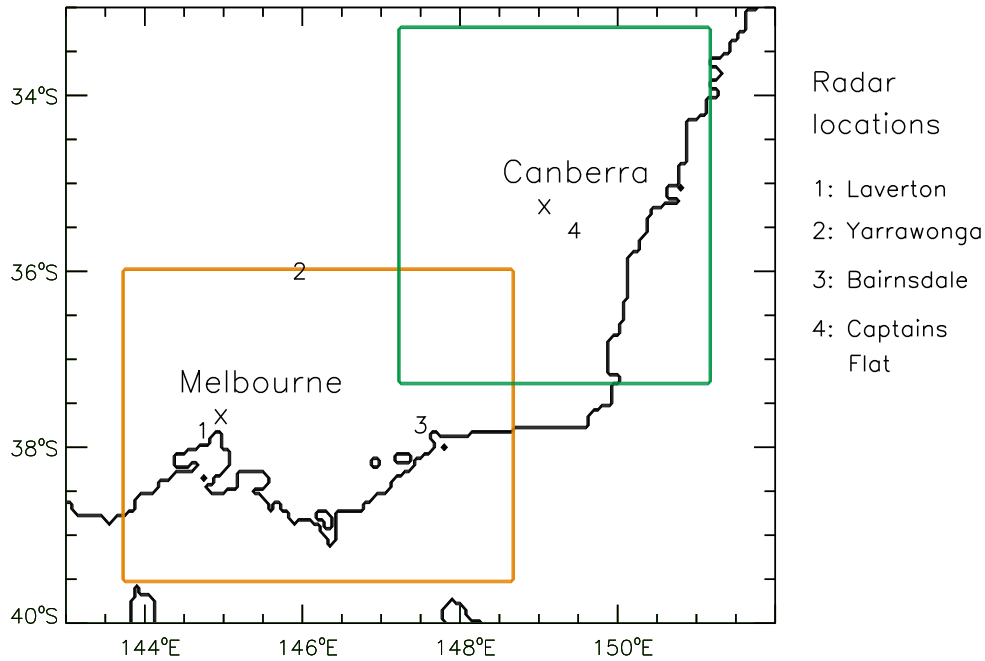
- 489 Latham, D. (1991), Lightning flashes from a prescribed fire-induced cloud, *J. Geophys. Res.*
490 *Atmos.*, 96(D9), 17151-17157.
- 491 Lindley, T., J. Vitale, W. Burgett, and M. Beierle (2011), Proximity Meteorological
492 Observations for Wind-driven Grassland Wildfire Starts on the Southern High Plains,
493 *Electronic-J. Severe Storms Meteor.*, 6(1), 1-27.
- 494 Luderer, G., J. Trentmann, and M. O. Andreae (2009), A new look at the role of fire-released
495 moisture on the dynamics of atmospheric pyro-convection, *Int. J. Wildland Fire*, 18(5),
496 554-562.
- 497 Luke, R. H., and A. G. McArthur (1978), Bushfires in Australia, AGPS Canberra, 359 pp.
- 498 McCaw, L., G. Mills, A. Sullivan, R. Hurley, P. Ellis, S. Matthews, M. Plucinski, B. Pippen, and
499 J. Boura (2009), Fire behavior investigation, Victorian 2009 Bushfire Research Response
500 Final Report.
- 501 McRae, R. H., J. J. Sharples, S. R. Wilkes, and A. Walker (2013), An Australian pyro-
502 tornadogenesis event, *Natural Hazards*, 65(3), 1801-1811.
- 503 McRae, R. H. D., J. J. Sharples, and M. D. Fromm (2015), Linking local wildfire dynamics to
504 pyroCb development, *Nat. Hazards Earth Syst. Sci.*, 15, 417-428, doi:10.5194/nhess-15-
505 417-2015.
- 506 Mills, G. A. (2005a), A re-examination of the synoptic and mesoscale meteorology of
507 AshWednesday 1983, *Aust. Meteorol. Mag.*, 54, 35-55.
- 508 Mills, G.A. (2005b), On the sub-synoptic scale meteorology of two extreme fire weather days
509 during the Eastern Australian fires of January 2003, *Aust. Meteorol. Mag.*, 54, 265-290.
- 510 Mills, G.A. (2008), Abrupt surface drying and fire weather Part 2: a preliminary synoptic
511 climatology in the forested areas of southern Australia, *Aust. Meteorol. Mag.*, 57(4).
- 512 Mills, G. A., and L. McCaw (2010), Atmospheric Stability Environments and Fire Weather in
513 Australia - extending the Haines Index. CAWCR Technical report No. 20. *Centre for*
514 *Australian Weather and Climate Research*.
- 515 Murphy, B. P., R. A. Bradstock, M. M. Boer, J. Carter, G. J. Cary, M. A. Cochrane, R. J.
516 Fensham, J. Russell-Smith, G. J. Williamson, and D. M. Bowman (2013), Fire regimes of
517 Australia: a pyrogeographic model system, *J. Biogeography*, 40(6), 1048-1058.
- 518 Peterson, D. A., E. J. Hyer, J. R. Campbell, M. D. Fromm, J. W. Hair, C. F. Butler, and M. A.
519 Fenn (2015), The 2013 Rim Fire: Implications for predicting extreme fire spread,
520 pyroconvection, and smoke emissions, *Bull. Amer. Meteorol. Soc.*, 96(2), 229-247.
- 521 Peterson, D. A., E. J. Hyer, J. R. Campbell, J. E. Solbrig, and M. D. Fromm (2016), A
522 Conceptual Model for Development of Intense Pyrocumulonimbus in Western North
523 America, *Mon. Weath. Rev.*, doi:10.1175/MWR-D-16-0232.1.
- 524 Potter, B.E. (2012a), Atmospheric interactions with wildland fire behaviour-I. Basic surface
525 interactions, vertical profiles and synoptic structures, *Int. J. Wildland Fire*, 21(7), 779-
526 801.
- 527 Potter, B. E. (2012b), Atmospheric interactions with wildland fire behaviour-II. Plume and
528 vortex dynamics, *Int. J. Wildland Fire*, 21(7), 802-817.

- 529 Pumphrey, H. C., M. L. Santee, N. J. Livesey, M. J. Schwartz, and W. G. Read (2011),
530 Microwave Limb Sounder observations of biomass-burning products from the Australian
531 bush fires of February 2009, *Atmos. Chem. Phys.*, 11(13), 6285-6296.
- 532 Reeder, M. J., and R. K. Smith (1987), A study of frontal dynamics with application to the
533 Australian summertime cool change, *J. Atmos. Sci.*, 44, 687-705.
- 534 Reeder, M. J., T. Spengler, and R. Musgrave (2015), Rossby waves, extreme fronts, and
535 wildfires in southeastern Australia. *Geophys. Res. Lett.*, 42(6),
536 doi:10.1002/2015GL063125.
- 537 Rorig, M. L., and S. A. Ferguson (1999), Characteristics of lightning and wildland fire ignition in
538 the Pacific Northwest, *J. App. Meteorol.*, 38(11), 1565-1575.
- 539 Rosenfeld, D., M. Fromm, J. Trentmann, G. Luderer, M. O. Andreae, and R. Servranckx (2007),
540 The Chisholm firestorm: observed microstructure, precipitation and lightning activity of a
541 pyro-cumulonimbus, *Atmos. Chem. Phys.*, 7(3), 645-659.
- 542 Rothermel, R. C. (1991), Predicting behavior and size of crown fires in the Northern Rocky
543 Mountains, Res. Pap. INT-438. Ogden, UT: U.S. *Department of Agriculture, Forest*
544 *Service*.
- 545 Russell-Smith, J., C. P. Yates, P. J. Whitehead, R. Smith, R. Craig, G. E. Allan, R. Thackway, I.
546 Frakes, S. Cridland, M. C. Meyer, and A. M. Gill (2007), Bushfires down under: patterns
547 and implications of contemporary Australian landscape burning, *Int. J. Wildland Fire*,
548 16(4), 361-377.
- 549 Siddaway, J. M., S. V. Petelina, A. Feofilov, A. Y. Zasetsky, A. R. Klekociuk, and J. Urban
550 (2010). UTLS hydration by the smoke plume from 2009 Australian Black Saturday
551 bushfire, In AGU Fall Meeting Abstracts (Vol. 1, p. 0059).
- 552 Sullivan, A. L., W. L. McCaw, M. G. Cruz, S. Matthews, and P. F. Ellis (2012), Fuel, fire
553 weather and fire behaviour in Australian ecosystems, *Flammable Australia: fire regimes,*
554 *biodiversity and ecosystems in a changing world*, CSIRO Publishing, Australia, 51-77.
- 555 Sullivan, A. L., and S. Matthews (2013), Determining landscape fine fuel moisture content of the
556 Kilmore East 'Black Saturday' wildfire using spatially-extended point-based models,
557 *Environmental Modelling and Software*, 40, 98-108.
- 558 Tosca, M. G., D. J. Diner, M. J. Garay, and O. V. Kalashnikova (2015), Human-caused fires
559 limit convection in tropical Africa: First temporal observations and attribution, *Geophys.*
560 *Res. Lett.*, 42(15), 6492-6501.
- 561 Victorian Bushfire Royal Commission (VBRC) (2009), Final Report, Volume 1, The Fires and
562 the Fire-Related Deaths, ISBN 978-0-646-51830-5.



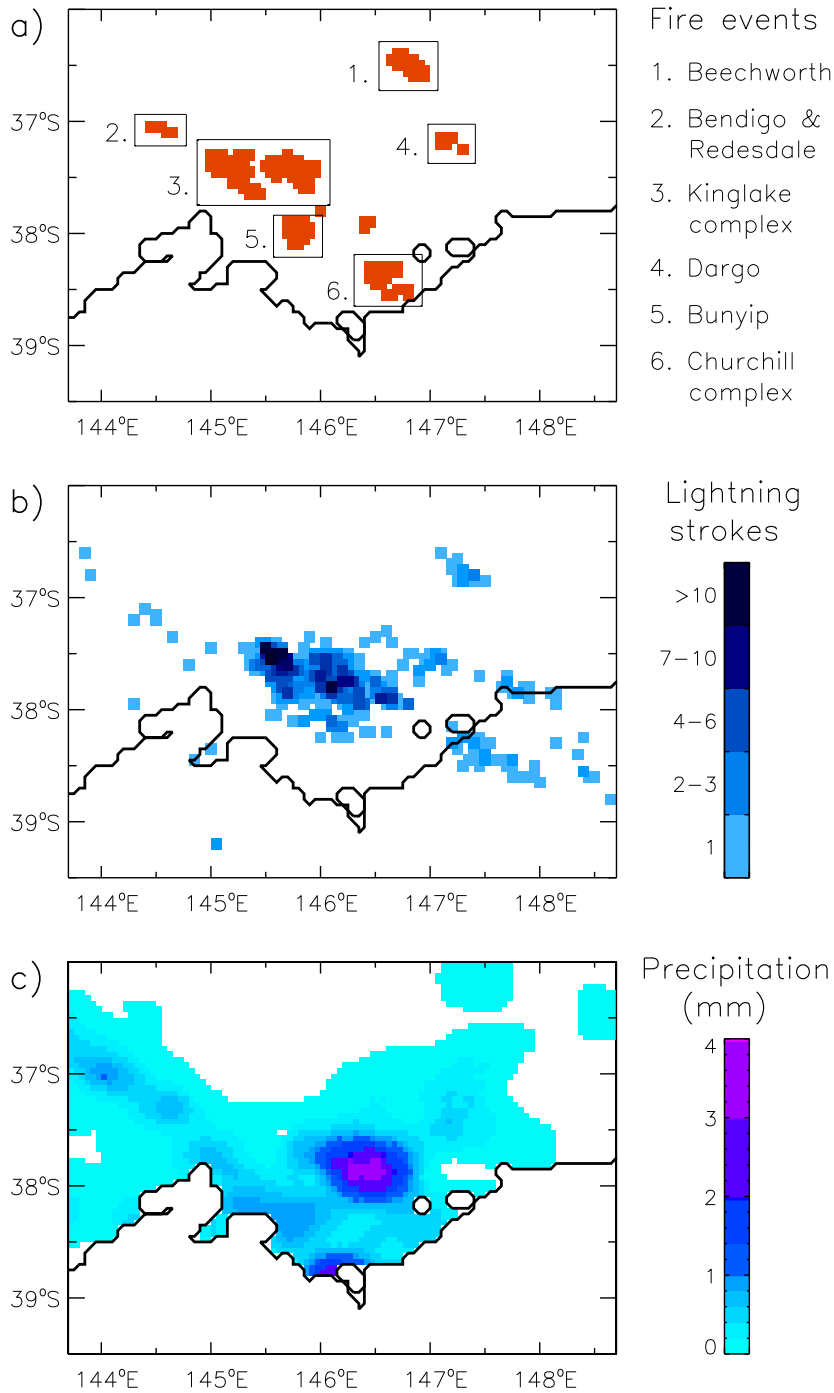
563

564 **Figure 1.** Synoptic features on Black Saturday, as represented by the Mean Sea Level Pressure
565 (MSLP) analysis produced operationally by the Bureau of Meteorology. This is shown for 2300
566 LT on 7 February 2009.



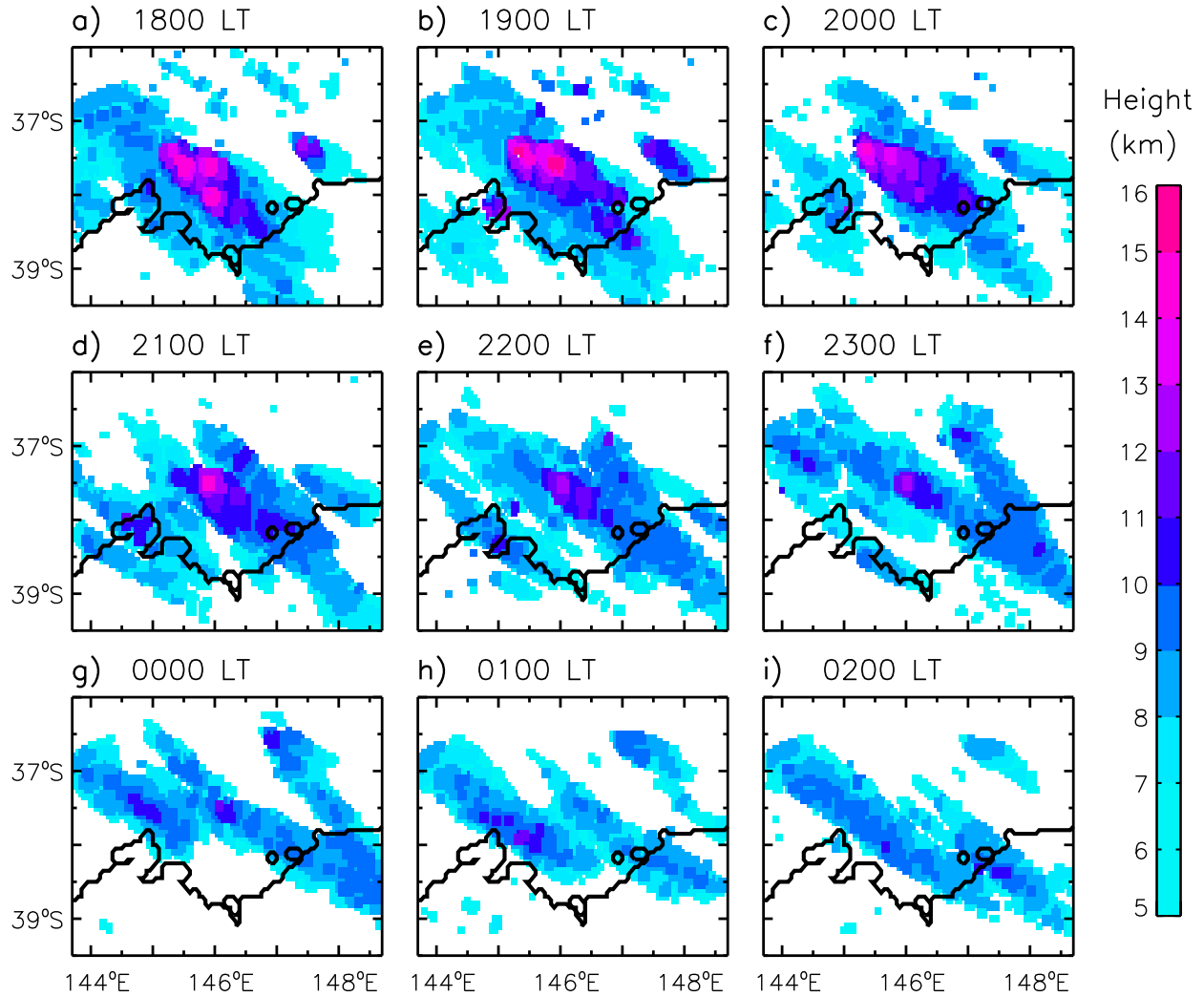
567

568 **Figure 2.** Map of southeast Australia showing cities (Melbourne and Canberra: 'x' symbols),
569 radar locations, coastlines, latitude and longitude. The inset boxes represent two regions of focus
570 for this study, for Black Saturday (orange box) and the Canberra fire event (green box),
571 respectively. The locations of radars referred to in this study are also shown.

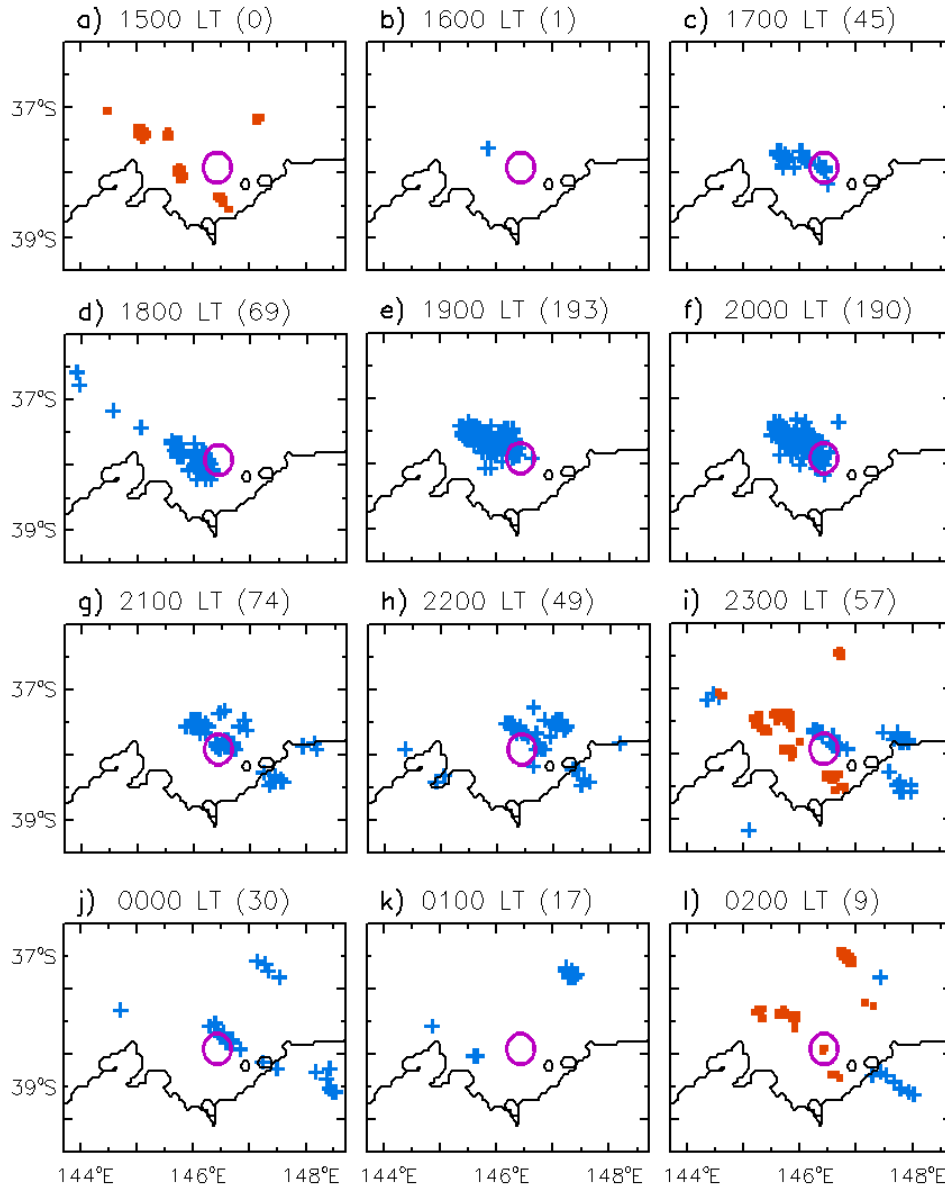


572

573 **Figure 3.** Fire, lightning and precipitation observations on Black Saturday. Active fire
 574 observations are shown, with six notable fire events listed (a). Lightning stroke counts (strokes
 575 per $0.05^\circ \times 0.05^\circ$ grid-cell) are shown based on observations obtained from a ground-based
 576 network of sensors (b). Precipitation data are based on a gridded analysis of observations over
 577 land (c). The fire and lightning data represent all observations within the time period from 1500
 578 LT on 7 February 2009 to 0300 LT on 8 February 2009, while the precipitation data are based on
 579 daily observations for the 24-hour time period from 0900 LT on 7 February 2009 to 0900 LT on
 580 8 February 2009. Coastlines, latitude and longitude are shown.

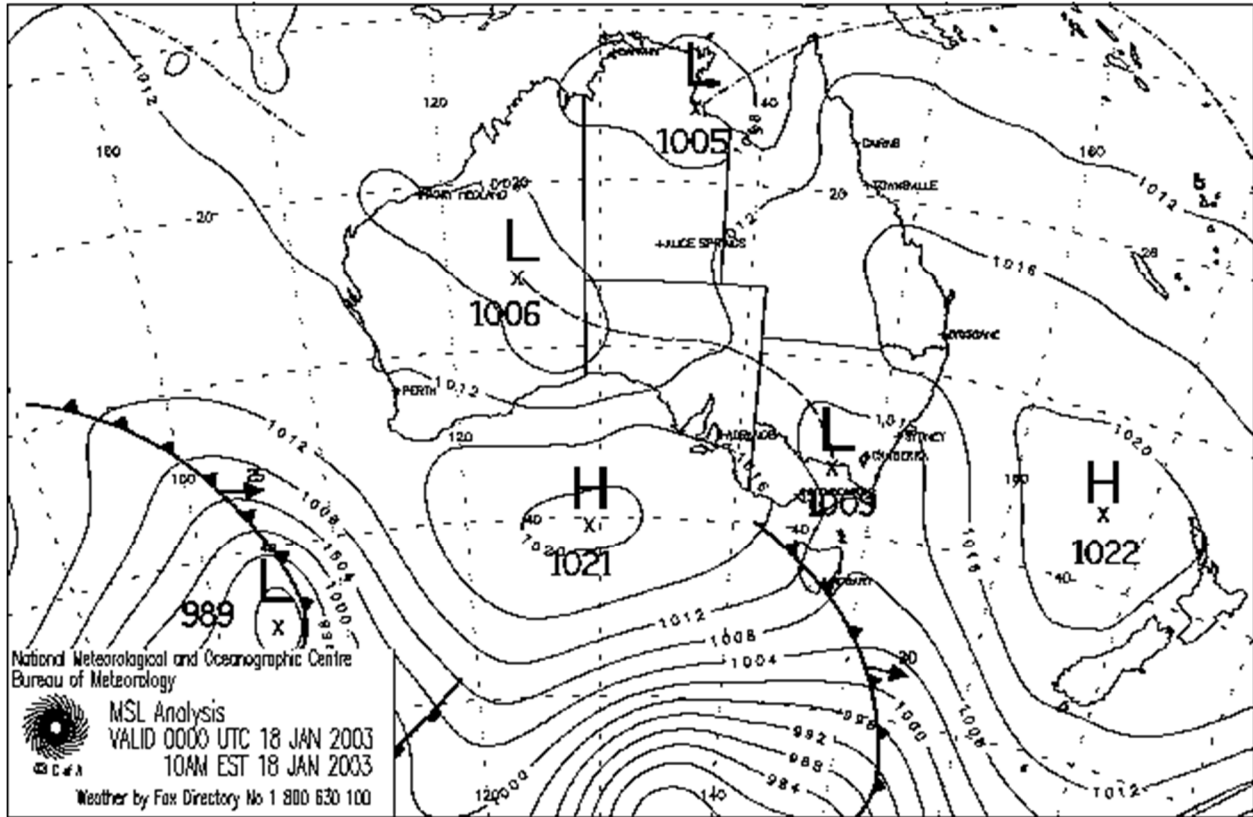


581
 582 **Figure 4.** Echo-top heights obtained from radar observations. Hourly values are shown from
 583 1800 LT on Black Saturday to 0200 LT the following day, representing the highest echo-top
 584 recorded during the 1-hour period starting from the time shown. Coastlines, latitude and
 585 longitude are shown.



586

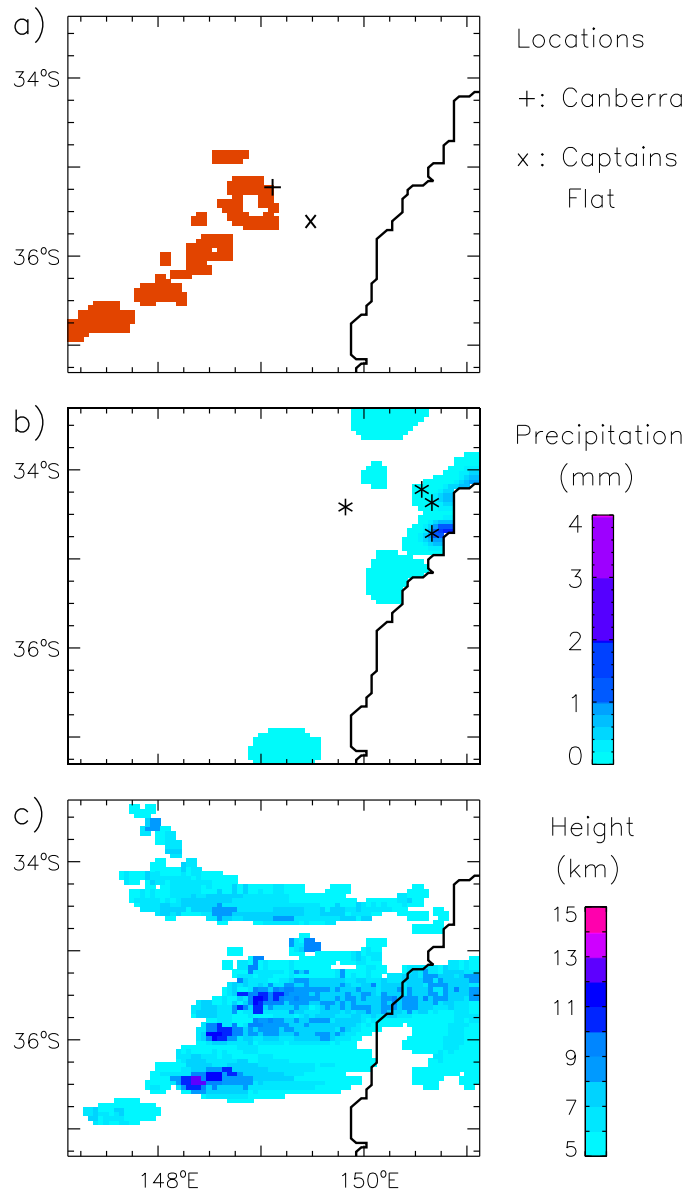
587 **Figure 5.** Temporal evolution of the lightning and fire activity. Lightning activity (blue '+'
 588 symbols) and active fire observations from satellite overpasses (red regions) are shown during
 589 the hours of 1500 LT and 2300 LT on 7 February 2009 as well as 0200 LT on 8 February 2009.
 590 Data are presented in hourly intervals from 1500 LT on 7 February 2009 to 0200 LT on 8
 591 February 2009 in panels a) to l), respectively, representing all observations within one-hour
 592 periods starting from the specified times. The hour is listed at the top of each panel, followed in
 593 brackets by the total number of lightning strokes recorded during that hour in the region shown.
 594 Coastlines, latitude and longitude are shown, as well as the location of a fire examined in relation
 595 to pyrogenic lightning ignition (purple circle) with the active fire observations for that case
 596 shown in panel l).



597

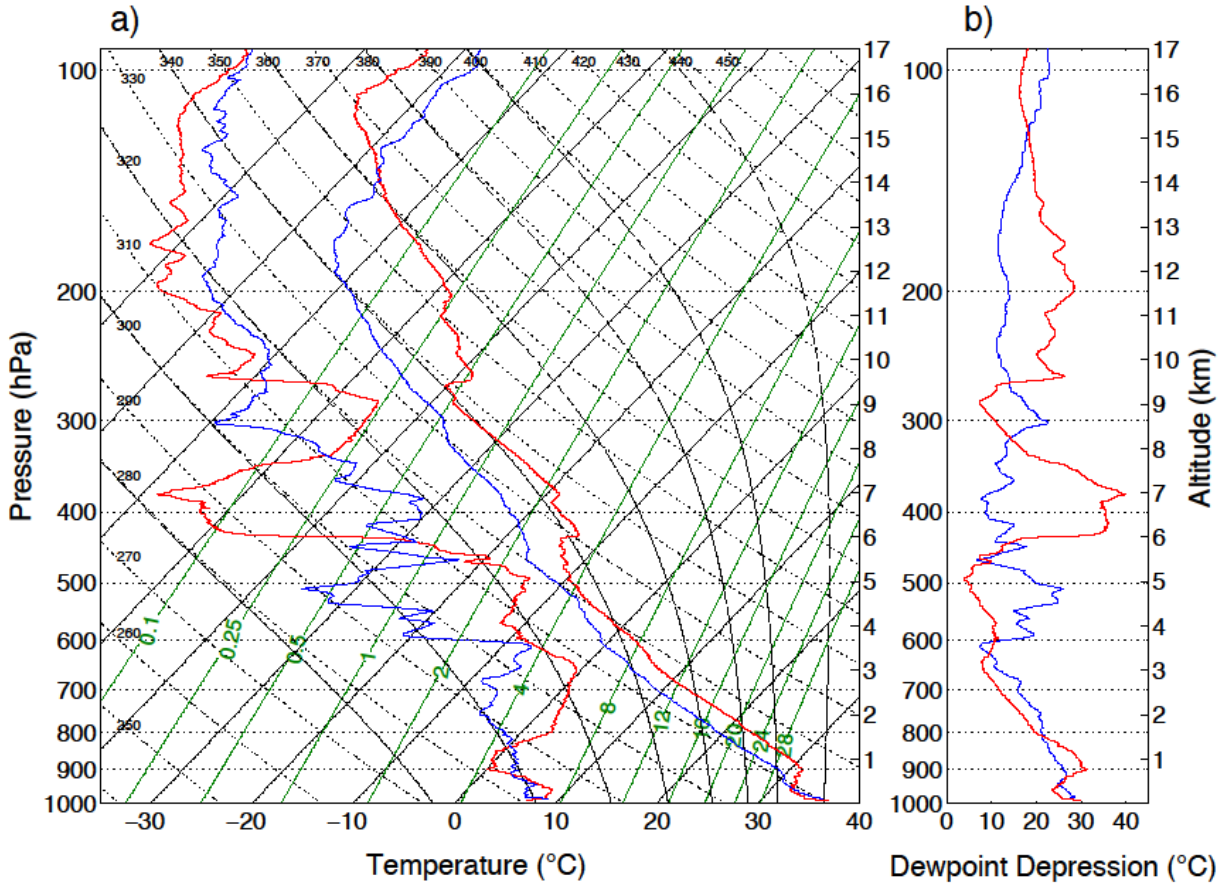
598 **Figure 6.** Synoptic features for the Canberra fire event, as represented by the Mean Sea Level
599 Pressure (MSLP) analysis produced operationally by the Bureau of Meteorology. This is shown
600 for 1100 LT on 18 January 2003.

601



602

603 **Figure 7.** Observations for the Canberra fire event, 18 January 2003 in the Australian Capital
 604 Territory: active fire observations (a), lightning ('*' symbols) and precipitation data (b), as well
 605 as echo-top heights from the Captains Flat radar (c). The fire and lightning data represent all
 606 observations within the period from 1500 LT on 18 January 2003 to 0300 LT on 19 January
 607 2003. Precipitation data are based on daily observations over land for the 24-hour time period
 608 from 0900 LT on 18 January 2003 to 0900 LT on 19 January 2003. Echo-top heights are for the
 609 period from 1800 LT on 18 January 2003 to 0200 LT on 19 January 2003. Coastlines, latitude
 610 and longitude are shown.



611

612 **Figure 8.** Radiosonde observations showing vertical profiles of temperature and dewpoint (a) as
 613 well as dewpoint depression (b). This is shown for the Canberra fire event (blue) based on
 614 observations from Wagga Wagga at 0000 UT on 18 January 2003, as well as for Black Saturday
 615 (red) based on observations from Melbourne Airport at 2300 UT on 6 February 2009.